BNL-102023-2014-TECH
AD/RHIC/111;BNL-102023-2013-IR

Time-Dependent Hydrogen and Helium Pressure Profiles in a Long, Cryogenically Cooled Tube, Pumped at Periodic Intervals

J. P. Hobson

August 1992

Collider Accelerator Department
Brookhaven National Laboratory

U.S. Department of Energy
USDOE Office of Science (SC)

DISCLAIMER

BNL–47434
AD/RHIC–111
Informal Report

Time-Dependent Hydrogen and Helium Pressure Profiles in a Long, Cryogenically Cooled Tube, Pumped at Periodic Intervals

J. P. Hobson and K. M. Welch

August 1992

RHIC PROJECT

Brookhaven National Laboratory
Associated Universities, Inc.
Upton, NY 11973

Under Contract No. DE–AC02–76CH00016 with the
UNITED STATES DEPARTMENT OF ENERGY

TIME-DEPENDENT HYDROGEN AND HELIUM PRESSURE PROFILES IN A LONG, CRYOGENICALLY COOLED TUBE, PUMPED AT PERIODIC INTERVALS*

J. P. Hobson
National Vacuum Technologies, Inc.
Ontario, Canada

and

K. M. Welch
RHIC Project
Brookhaven National Laboratory

ABSTRACT

Many particle accelerators and colliders throughout the world make use of superconducting magnets to focus highly relativistic beams. These magnets are cooled to ~ 4.2° K. For practical reasons, the beam pipes, encircled by the magnets, also operate at these cryogenic temperatures. This paper presents a theoretical model for determining pressure profiles, in space and time, stemming from either hydrogen or helium gas leaks into the cold-bore tube with appendage pumps located at periodic intervals. It is shown that a wave-like pressure gradient propagates from the leak source at a rate which is dependent on the leak magnitude, gas species, speed and location of appendage pumps, and the geometry and effective roughness of the cold-bore tube. Steady-state, linear pressure gradients eventually equilibrate between the appendage pumps in a magnitude commensurate with both the adsorption isotherm of the species and mass flow in the beam pipe. Results are given for a variety of conditions relevant to the Relativistic Heavy Ion Collider being constructed at Brookhaven, and a general procedure, with expressions, is provided for the making of similar calculations in other installations.

* Work supported by the United States Department of Energy.

Introduction

The objective of the Relativistic Heavy Ion Collider (RHIC) project is do physics research involving the collisions of highly relativistic particle beams. The RHIC machine, described elsewhere and presently under construction,[1] must store two counter-rotating particle beams for periods of greater than ten hours. Colliding beams may comprise protons, gold ions (i.e., Au^{+79}), or a variety of heavy ions, colliding with each other or protons.

First, the intensity, and thus usefulness, of the particle beams is diminished when the stored particles are lost from their contrived orbits either due to charge exchange processes or through nuclear scattering with background gas. Secondly, particle beam collisions with gas in regions near the experimental detectors cause background *noise* in these detectors, and are therefore undesirable. For these and other reasons, a low operating pressure in the RHIC is very important. The RHIC, illustrated in Fig. 1, comprises two interweaving *rings* ~3.8 km in circumference. About seventeen percent of the life of each beam is spent in *warm*, RT (i.e., room temperature) sections of the rings; the remainder is spent in beam pipe operating at a temperature of ~4.2° K (i.e., the *cold-bore*). An average total pressure of $\leq 5 \times 10^{-10}$ Torr is required in the warm sections, the gases comprising 90% H_2, 5% CO and 5% CH_4. However, the pressure specification for beam components such as kickers, septum and RT rf cavities is $\leq 2 \times 10^{-9}$ Torr, in the same gas species proportions. The requirement for the average total pressure of the cold-bore is $\leq 10^{-11}$ Torr, comprising exclusively H_2 and He. Maintenance of the above pressures assure adequate beam life-times and acceptable beam-emittance growth rates.

Helium and Hydrogen Problem Sources

It was thought prudent in the construction of the RHIC machine to require that no welded, brazed or bolted vacuum joints serve as barriers between LHe (i.e., liquid helium) and UHV environments. This is because 4.2° K LHe-I has a factor of $\sim 10^{+2}$ greater leak rate through an equivalent RT, gaseous He leak. Liquid helium cryogen, separately plumbed from one magnet to the next, is pumped through holes in the 6.4 mm thick, stacked laminations of the various superconducting magnets. Welded stainless steel shells, containing and aligning the magnet laminations, serve as LHe barriers from the cryostat insulating vacuum. This is a necessary compromise. However, the cold-bore comprises a seamless, austenitic stainless steel tube, extending beyond the end-plates of the magnets to which it is welded. The UHV cold-bore is interconnected between magnets with formed bellows. Therefore, the only means whereby He can leak into the cold-bore UHV system is through metallurgical flaws in the seamless pipe, because of possible damage caused during the welding of the beam pipe to the magnet end-

plates, or from the circumstance of gaseous He, in the cryostat, leaking through a catastrophic failure in the UHV interconnect piping or bellows.

Several possible sources of hydrogen exist and will be pumped by the cold-bore. First, there are end-effects from the warm sections and RT beam components proximate to the cold-bore (e.g., see Fig 2). Roughly 50 such temperature transition regions exist in the RHIC. For extremely high energy machines, having synchrotron radiation, H_2 is synthesized within the cold-bore as the result of the dissociation, by desorbed photoelectrons, of cryocondenced H_2O resident on the inner walls of the cold-bore. This becomes a distributed pumping problem as it involves a distributed gas source. Lastly, H_2 may evolve from dissociation of H_2O by unbaked RT instrumentation used to monitor cold-bore pressures. The motivation for this work is to be able to predict possible He or H_2 pressure gradients in the cold-bore tubes resulting from *leaks*, and to be able to accommodate and measure such leaks.

The Theoretical Model

Observations of Edwards and Limon played a major role leading to the construction of our theoretical model.[2] They noted that when introducing a large He leak into one end of a 6 cm ϕ cold-bore tube, cooled to 4.7° K, it took approximately 2.5 minutes before a He pressure increase was noted in the cold-bore, 20 m removed from the leak. After the 2.5 minutes, the He pressure abruptly increased at the remote gauge. From this they concluded: "It perhaps can be thought of as a high-pressure helium front slowly migrating down the tube." This led to the assumptions made in constructing the model for He or H_2 leaks somewhere within the linear bounds of a cold-bore tube. The assumptions are as follows:

#1. The inlet gas initially has the same probability of coursing longitudinally in either direction in the cold-bore from the leak location.

#2. Under all conditions pressure gradients are linear with distance along the cold-bore, though varying in magnitude with the use of pumps.

#3. The surface population density of gas species along the cold-bore, σ, is consistent with an adsorption isotherm of the species stemming from the linear pressure gradients.

#4. When lumped pumps are distributed along the cold-bore, it is assumed that these pumps have no inherent capacity limitations.

#5. No gas reaches a lumped pump until the *foot* of the linear pressure wave reaches that pump. Thereafter, pressure gradients between pumps are consistent with the throughput in the cold-bore and pump speeds. That is, $d^2P/dx^2 = 0$, at all times in the process except at the singularity points of gas sources and sinks.

The above assumptions must take into consideration thermal transpiration effects when calculating cold-bore gas densities resulting from gas entering therein from the warm-bore. That is, the maximum possible gas density within the cold-bore, ρ_c, stemming from end effects of the warm-bore, will always be $\rho_c \leq (293^\circ K/4.2^\circ K)^{0.5}\ \rho_w \approx 8.35\ \rho_w$, where ρ_w is the gas density in the warm-bore. Therefore, this represents a time-varying leak rate into the cold-bore, and this *leak* eventually decays to zero.

With the above assumptions, solution of the problem is simply one of counting molecules; that is, doing the arithmetic to make sure that the surface population of the cold-bore and gas pumped by the lumped pumps is consistent with the amount of gas which has leaked into the cold-bore.

Background Data

It is required that we be able to predict surface gas population as a function of pressure. The measure of surface coverage is often given as:

$$\Theta = \sigma/\sigma_m, \qquad (1)$$

where, σ = the number of atoms or molecules per cm^2,
and, = one monolayer, or *Langmuir.*

For helium, $\sigma_m = 7.22 \times 10^{14}$ atoms/cm^2, and for hydrogen, $\sigma_m = 6.95 \times 10^{14}$ molecules/cm^2.[3] The value of Θ is found by the following:[3]

$$\ln\Theta = -B(RT\ln(P/P_0))^2, \qquad (2)$$

where, B_{He} = 4.01×10^{-5} cal^{-2} $mole^2$,[4]
B_{H_2} = 3.59×10^{-6} cal^{-2} $mole^2$,[5]
P = pressure over the surface gas, in Torr,
$P_{0,He}$ = 760 Torr He,
P_{0,H_2} = 1.044×10^{-6} Torr H_2,[6]
R = 1.986 cal/mole °K,
and, T = 4.2° K.

The exact equations of the boundary value problem are:[7]

$$dQ(x,t) = -P(x,t)(S(\Theta,t)/x_0)dx, \qquad (3)$$

$$dP(x,t) = -Q(x,t)(Cx_0)^{-1}dx, \qquad (4)$$

$dQ(x,t)$ = the gas throughput into the cold-bore,
$S(\Theta,t)/x_0$ = the cold-bore pumping speed per unit length,
$(Cx_0)^{-1}$ = the cold-bore impedance per unit length,
t = the time in seconds.
x = the distance along the cold bore.

We have not attempted to solve this boundary value problem. Rather, we have used numerical approximations and the noted assumptions.

General Expression For Wave Propagation

Assume for the moment that the cold-bore serves as the only pump. Calculated values of Θ *vs.* P are given for He and H_2 in Fig. 3 and Fig. 4, respectively. It is convenient to express Θ in an approximate form which is more readily integrable so as to be able to derive an analytical expression for the wave front velocity, location and magnitude in the cold-bore. Such an approximation is given by:

$$\Theta \sim k_1 P^n. \tag{5}$$

Equation (5), a reasonable *fit*, is plotted as dashed lines in Figures 3 and 4, where values k_1 and n are also given for He and H_2 at 4.2° K. Note that the values of k_1 and n vary depending on the cold-bore temperature.

Assumption #3 implies that the cold-bore serves as a pump of speed equivalent to that of the aperture of the cold-bore for the given species and temperature. The unique aspect of this pump is that it *moves* along the tube at the *foot* of the wave front established by gas accumulated on the cold-bore. A major portion of the RHIC cold-bore inside diameter is, $D \sim 6.9$ cm ϕ. This implies that the *moving-pump* speed is $C_a \sim 140$ ℓ/sec for He, and $C_a \sim 200$ ℓ/sec for H_2 at 4.2° K. Further, the speed delivered at the leak location, C, as a consequence of the C_a, at a distance x, is given by:[8]

$$C = \frac{C_a}{(1 + 0.75\,x/D)}, \tag{6}$$

C = cold-bore conductance, ℓ/sec,
C_a = $C_{He} \approx 140$ ℓ/sec,
or , = $C_{H_2} \approx 200$ ℓ/sec,
L = the length of the cold-bore in centimeters,
D = the diameter of the cold-bore in centimeters.

For a leak of $2 \times Q$ Torr-ℓ/sec, the pressure at the leak, $P_{o,t}$, is assumed to be:

$$P_{o,t} = Q/C\ , \tag{7}$$

where the pressure downstream of the leak is given by:

$$P(x) = Q/C_a. \tag{8}$$

Equation (6) has some very interesting properties. As $x \to 0$, $C \to C_a$. And, for large values of x, C approaches the *long-tube* value subtended by C_a.

Using (5) through (8), and the given assumptions, we develop a general expression for the amount of gas stored in the cold-bore at any time, t, as:

$$Q \times t = \frac{\pi \sigma_m D r \Re T}{N_o} \int_0^x \Theta(x)dx, \tag{9}$$

$$\sim \frac{\pi \sigma_m D r \Re T}{N_o} k_1 \int_0^x P(x)^n dx, \tag{10}$$

$$\sim \frac{k_1 k_2}{(n+1)b} \{(a + bx)^{(n+1)} - (a)^{(n+1)}\}, \tag{11}$$

where, $k_2 = \frac{\pi \sigma_m D r \Re T}{N_o}$

Q = half the leak throughput in Torr-ℓ/sec,
t = the time in seconds,
x = location of the wave front, in centimeters,
D = the cold-bore diameter in centimeters,
r = the internal roughness factor of the cold-bore,
$\Re$ = 63.26 Torr-ℓ/mole° K,
T = cold-bore temperature in ° K,
N_o = Avogadros number,
a = $P_{o,t}$, the pressure at the leak (*i.e.*, at $x = 0$), in Torr,
b = $(P_x - P_{o,t})/x$,
and, P_x = the pressure at the wave-front, in Torr.

Using (11), we can derive an expression for the velocity, in cm/sec, with which the foot of the wave-front moves along the cold-bore. This is given by:

$$\frac{\Delta x}{\Delta t} = \frac{Q (P_{o,t} - P(x)) (n+1)}{k_1 k_2 x} \div \frac{\Delta^2 P(x)^{(n+1)}}{\Delta x \Delta t} \tag{12}$$

On substituting for k_2 in (12), the component "1/T" stems from the Universal Gas Law, rather than from the physics of the wave velocity. Actually, numerical evaluation of (12) shows that, as one would expect, dx/dt increases with T. Other than this, we note that dx/dt is directly proportional to Q, and inversely proportional to D and r. These results are equally intuitive. The inverse relationship of r has some very important implications. For example, assume the inside of a cold-bore is plated with a material having an effective surface area of ×1000 that of the projected area. Propagating waves will have identical features on reaching the same location in both the plated and unplated

pipes. However, in the case of the plated cold-bore pipe, the time it takes for the foot of the wave to reach a given location is ×1000 greater!

Figures 5 and 6 graphically summarize results of (12) for a cold-bore diameter of 6.9 cm, at a temperature of 4.2° K and for different H_2 and He leak rates, respectively. Only two aspects are particularly interesting about the difference between the He and H_2 data. First, the He wave-front appears to decelerate more rapidly with distance than the H_2 wave-front. Secondly, the H_2 wave-front appears to progress much more slowly than that of the He wave-front, for the same Q. This we would expect as H_2 is much more *sticky* on 4.2° K surfaces than He. We will return to these figures in later calculations.

Pumps Distributed Along the Cold-Bore

There are no *neat*, closed equations which express the pressure along a cold-bore of diameter D, with pumps of speed S, spaced at intervals L. Figure 7 illustrates such a system. The graphs shown above the cold-bore manifold represent *snapshots* of the locations and magnitudes of a He wave-front at times 0+, 1, 1+ and 2. The numbers along the abscissa of each graph represent locations of pumps along the cold-bore. The ordinate of the graphs give the pressure of the wave at various locations along the cold-bore. For example, $P_{x,t}$ is the pressure in the cold-bore at location x and at time t. Our model assumes that until the wave-front reaches a particular pump, that pump has no effect on the wave. However, once the wave overtakes the pump, that pump and all pumps between it and $x = 0$ play a role in defining the pressure gradients.

The arithmetic of this case is slightly more complicated than that of a wave propagating in a cold-bore with no lumped pumps. In order to predict the wave magnitude and location in time, we must keep track of the amount of He pumped by the various pumps in time, as well as that He *stored* on the cold-bore surface. Simply put, the population of gas on the cold-bore and the amount of gas pumped by the lumped pumps, both up to time t, must be consistent with the product $Q \times t$, where Q is again half the leak throughput.

Assume that the speed of each lumped pump is the same, and has the value S. At time t_2, half of the leaking gas is accounted for by:

$$Q \times t_2 = k_2 \int_0^2 \Theta(x)dx + (S/2)(P_{1,2} + P_{1,1})(t_2 - t_1) \quad (13)$$

$$= k_1 k_2 \int_0^2 P(x)^n + (S/2)(P_{1,2} + P_{1,1})(t_2 - t_1)$$

The second term on the right of (13) is the amount of gas pumped by the

pump at location 1 in the time interval $(t_2 - t_1)$. The value t_1 is simply the time it takes the wave-front to reach the first pump. The value t_2 is the time it takes the wave-front to reach location 2. We solve (13) for t_2 as all other values are known. Similarly, when the wave-front reaches 3:

$$Q \times t_3 = k_2 \int_0^3 \Theta(x)dx + (S/2)(P_{1,2} + P_{1,1})(t_2 - t_1) + (S/2)(P_{1,3} + P_{1,2} + P_{2,3} + P_{2,2})(t_3 - t_2) \qquad (14)$$

This process is repeated as the wave-front progresses down the cold-bore. Figure 8 shows P(x) for different waves which have progressed ~100 m in the cold-bore from a leak of magnitude 10^{-n} Torr-ℓ/sec. It shows the cases of pumps spaced at 15 and 30 m intervals, for pumps with speeds of 1 and 5 ℓ/sec, and with no pumps. Obviously, these *snapshot* wave profiles occur at different times. For example, with a He leak of 10^{-8} Torr-ℓ/sec, and with no pumps, the wave-front will extend ~100 m from the leak in ~31 days, and the average pressure over this interval will be $\sim 1.0 \times 10^{-8}$ Torr. On the other hand, with lumped pumps having speeds of 5 ℓ/sec and spaced at 15 m intervals, the wave will take $\sim 2.3 \times 10^4$ days to travel 100 m, and the average pressure over this interval will be $\sim 2.7 \times 10^{-10}$ Torr.

Figure 9 shows the time required for the wave-front to reach ~100 m for the five cases given in Fig. 8, and for a leak rate of 10^{-n} Torr-ℓ/sec. Of course, our primary concern is the average RHIC pressure in the cold-bore beam pipe, and what this will be as a function of time and leak rate. We can predict this for the case of no pumps, and for the gases H_2 and He, from Figures 6 and 7, respectively.

Because of fixed spacings between the RHIC magnets, it is most likely that we will pump the cold-bore with 5 ℓ/sec pumps, spaced at 30 m intervals. Bayard-Alpert gauges will append the cold-bore tube at alternate 30 m spacings. Figure 10 illustrates estimated RHIC gold beam lifetimes, in time, for the case of one He leak of various possible leak rates, and with 5 ℓ/sec pumps and without the use of cold-bore pumps.[9]

Lastly, it is important to be able to predict the amount of He pumped by the lumped pumps. Assuming 5 ℓ/sec pumps distributed at 30 m intervals, Fig. 11 summarizes the amount of He pumped by two pumps downstream from a leak as a function of leak rate, time and pump location with respect to the leak of magnitude 10^{-n} Torr-ℓ/sec. It is evident from work reported elsewhere that small sputter-ion pumps are probably unsuitable for this application.[10]

Hydrogen Sources

We will first examine the amount of H_2 pumped by the cold-bore as a consequence of dissociation of H_2O by the ~250 Bayard-Alpert gauges (BAGs) used to measure the cold-bore pressure in both rings. First, assume that the partial pressure of H_2O in these BAGs is $\sim 10^{-9}$ Torr (i.e., worst case). Assuming a BAG sensitivity of 20 per Torr and 4 mA emission, and that the proportion of H_2 created by the BAGs is one percent of the H_2O pressure, we would expect a continuous hydrogen flux of 2.3×10^{-15} Torr-ℓ/sec to emanate from each gauge. There are 125 BAGs in each 3.8 km ring. Assume the H_2 source is actually greater by $\times 400$. Then the total outgassing from each BAG is $\sim 10^{-12}$ Torr-ℓ/sec. Using Fig. 6, we see that in about 160 days the average pressure of one of the RHIC rings will incrementally increase by $\sim 7 \times 10^{-16}$ Torr as a consequence of the 125 BAGs. Obviously, H_2O dissociation by the BAGs proves of no consequence.

Hydrogen End Effects

We will model this circumstance for the case assuming no cold-bore pumps, and for comparatively short sections of cold-bore tube subtended on each end by warm-bore tubes. This might represent the case of the D8 cryostat, noted at the top of Fig. 2, or perhaps the Q3 to D0 cryostats noted to the right of the same figure. In most cases, there will be some form of beam component in the warm sections. These might include rf cavities, kickers, beam dumps, septum, etc. The warm and cold sections are isolated from each other by the use of all metal valves. To preserve the quality of the baked, warm section vacuum systems, the valves between the warm and cold sections are opened only after the cold sections have achieved low temperatures. On opening the an isolation valve, the transient pumping of the warm beam component by the cold-bore tube will be as illustrated in Fig. 12. Even with the use of our simple model, the arithmetic of dealing with this transient case becomes formidable. For this reason, we will use the further simplification of assuming that the pressure within the short section of cold bore is uniform at all times. With these assumptions, on opening the valve at time $t = 0$:

$$Q_b = P_{b,o} (S_b + C_{aw}), \qquad (15)$$

where, Q_b = the beam component outgassing rate in Torr-ℓ/sec,
$P_{w,o}$ = the RT pressure in the beam component, in Torr,
S_b = the beam component pump speed, in ℓ/sec,
and, C_{aw} = the RT conductance of the warm-to-cold aperture.

Define $P_{w,t}$ as the pressure in the RT beam component vs. time, and $P_{0,t}$ as the pressure in the cold-bore at time t. When,

$$P_{w,t} = (T_w / T_c)^{0.5} P_{0,t} \quad (16)$$

where, T_c = the temperature of the cold-bore, in ° K,
and, T_w = the temperature of the warm section, in ° K,

the net flux of gas passing the cold-bore entrance aperture will be zero. Also, define $P_{b,c} = (T_c / T_w)^{0.5} P_b$, where P_b is the steady-state pressure in the beam component prior to opening the isolation valve. Therefore, the Q at time t going into the cold-bore is expressed by:

$$Q_{0,t} = C_{wa}[1 - (P_{0,t} / P_{c,b})] P_{0,t} \quad (17)$$

Assume that $P_{0,t}$ is given by the following:

$$P_{0,t} = P_{bc}(1 - ie^{-jt}), \quad (18)$$

where i and j are real numbers. The total Q at any time is constant and given by the following:

$$Q(t) = ((T_w / T_c)^{0.5}) \{S_b P_{0,t} + C_{wa}[1 - (P_{0,t} / P_{bc})] P_{0,t}\} \quad (19)$$

Substituting (18) into (19), and evaluating (19) as $t \to 0$, yields:

$$i = (C_{wa} - S_b) / C_{wa} \quad (20)$$

Using the above assumptions we solve the transcendental expressions coming from the following integration:

$$\int_0^t Q_{0,t}\, dt = k_2 \int_0^x \Theta(x,t) dx, \quad (21)$$

$$P_{bc} C_w (i/j)\{1 - e^{-jt} + (i/2)(e^{-2jt} - 1)\} = k_1 k_2 (i P_{0,t})^n x$$

Unique solutions of this transcendental equation indicate that for $x = 5$ m (i.e., half way through the short cold-bore section), and $S_b = 1000$ ℓ/sec, the cold-bore pressure will reach a pressure of $\sim 2.4 \times 10^{-10}$ Torr in ~11 hours. Remember, that a cold-bore pressure of this magnitude corresponds, in terms of gas density, to a warm-bore pressure of $\sim 1.7 \times 10^{-8}$ Torr. Should there be 25 such temperature transition regions in one RHIC ring, the effective lifetime of a gold beam would be reduced to ~100 hours without the benefit of some form of cold-bore pumping. Of course, these calculations neglect hydrogen end effects in the much longer magnet cryostats.

Conclusions

We have modeled a plausible mechanism for the propagation of He and H_2 waves in a cold-bore tube at cryogenic temperatures. We have given results of calculations for the cases including no pumps, and with lumped pumps, of different sizes distributed at different intervals along the cold bore. We have given a general expression for the velocity of wave propagation as a function of a wide variety parameters. If we use our model and *force-fit* the pressure at the leak to be $\sim 2.5 \times 10^{-4}$ Torr when the wave reaches ~20 m, as reported in the Edwards and Limon experiment, we calculate that our model would predict it took ~1.7 minutes, rather than ~2.5 minutes, for the wave to propagate that distance. Either there is a remarkable coincidence of agreement, or our model has some validity. It is hoped that this model will serve as a starting point to others attempting to make similar determinations.

References

1. Ozaki, S., "RHIC Project", IEEE Particle Accelerator Conference, Accelerator Science and Technology 5(5), 2901(1991).
2. Edwards, D., Jr., Limon, P., "Pressure Measurements in a Cryogenic Environment", J. Vac. Sci. Technol., 15(3), 1186(1978).
3. Redhead, P.A., Hobson, J.P., Kornelsen, E.V., The Physical Basis of Ultrahigh Vacuum (Chapman and Hall, Ltd., London, 1968).
4. Hobson, J.P., "First Adsorbed Layer of Helium at 4.2 K", Can. J. Phy. 37, 300(1959).
5. Halama, H.J., Aggus, J.R., "Cryosorption Pumping for Intersecting Storage Rings", J. Vac. Sci. Technol., 12, 532(1975).
6. Lee, T.J., "The Condensation of H_2 and D_2: Astrophysics and Vacuum Technology", J. Vac. Sci. Technol. 9(1), 257(1972).
7. Welch, K.M., Capture Pumping Technology, An Introduction (Pergamon Press, Oxford, 1991), p. 140.
8. Chambers, A., Fitch, R.K., Halliday, B.S., Basic Vacuum Technology (Adam Hilger, New York, 1989), p. 43.
9. Rhoades-Brown, M.J., Harrison, M., "Vacuum Requirements for RHIC", Informal Report #BNL-47070, December 1991.
10. Welch, K.M., Pate, D.J., Todd, R., Vitkun, K., "The Pumping of Hydrogen and Helium by Sputter-Ion Pumps", Invited Paper, 39th National AVS Symposium, Chicago, Ill., November 1992.

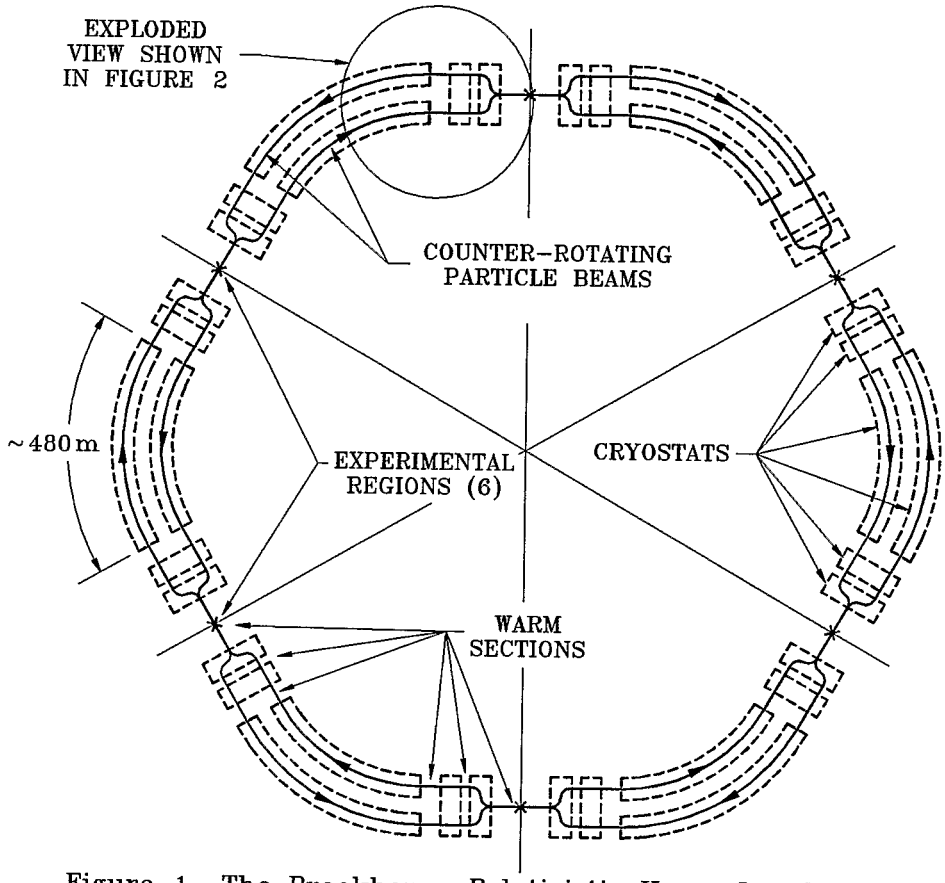

Figure 1. The Brookhaven Relativistic Heavy Ion Collider.

Kimo M. Welch
"rhicring"
0.4=1; 1.5,2

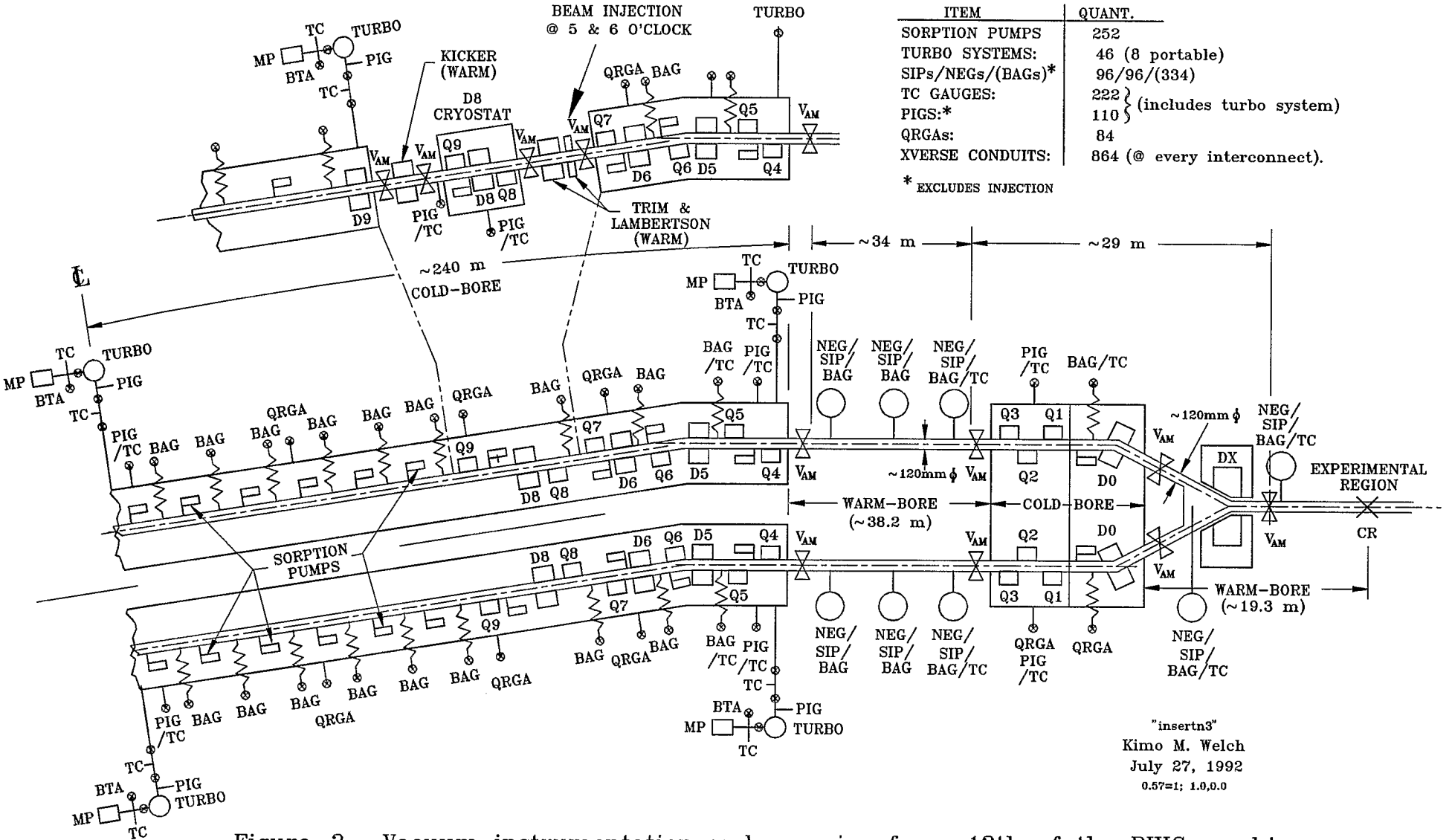

ITEM	QUANT.
SORPTION PUMPS	252
TURBO SYSTEMS:	46 (8 portable)
SIPs/NEGs/(BAGs)*	96/96/(334)
TC GAUGES:	222 } (includes turbo system)
PIGS:*	110 }
QRGAs:	84
XVERSE CONDUITS:	864 (@ every interconnect).

* EXCLUDES INJECTION

Figure 2. Vacuum instrumentation and pumping for a 12th of the RHIC machine.

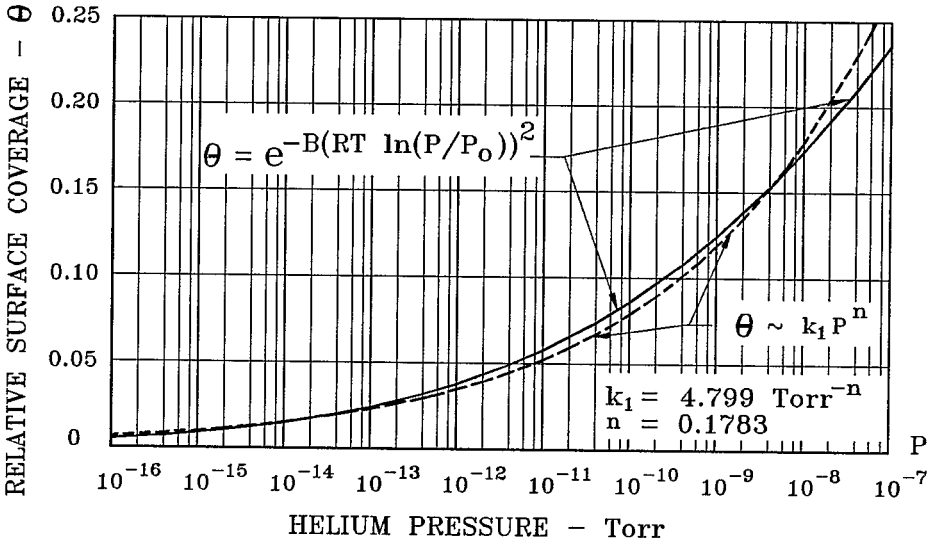

Figure 3. Helium Adsorption Isotherm at 4.2 °K.

kimo
"heh2isot"
1.5,3; 0.45=1

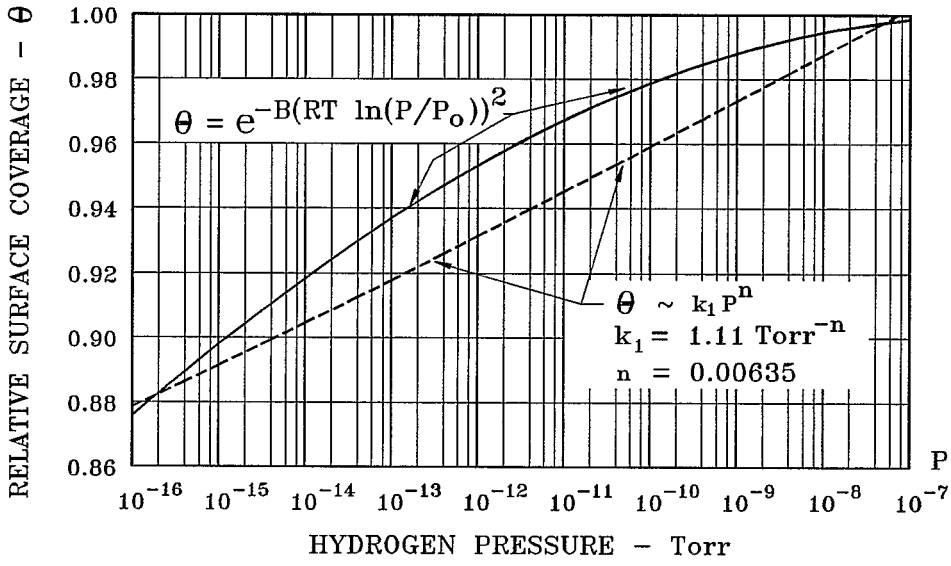

Figure 4. Hydrogen Adsorption Isotherm at 4.2°K.

kimo
"heh2isot"
1.5,3; 0.45=1

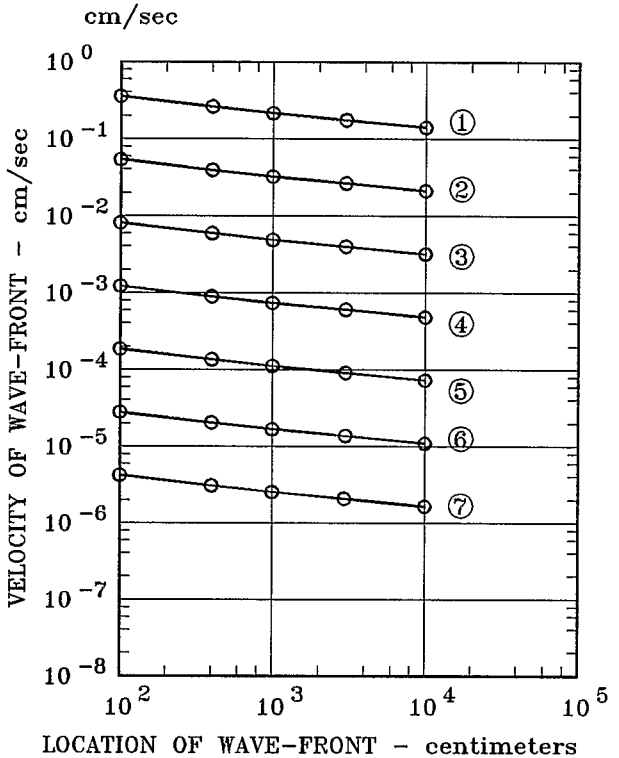

Q Total Torr-L/sec	Wave-Front Location-cm	Time to x - days	Average Interval Pressure - Torr
① 10^{-6}	10^2	$3.2*10^{-3}$	$4.3*10^{-8}$
	10^3	$4.7*10^{-2}$	$2.0*10^{-7}$
	10^4	$7.0*10^{-1}$	$2.0*10^{-6}$
② 10^{-7}	10^2	$2.1*10^{-2}$	$4.3*10^{-9}$
	10^3	$3.1*10^{-1}$	$2.0*10^{-8}$
	10^4	$4.6*10^{0}$	$2.0*10^{-7}$
③ 10^{-8}	10^2	$1.4*10^{-1}$	$4.3*10^{-10}$
	10^3	$2.1*10^{0}$	$2.0*10^{-9}$
	10^4	$3.1*10^{1}$	$2.0*10^{-8}$
④ 10^{-9}	10^2	$9.4*10^{-1}$	$4.3*10^{-11}$
	10^3	$1.4*10^{1}$	$2.0*10^{-10}$
	10^4	$2.0*10^{2}$	$2.0*10^{-9}$
⑤ 10^{-10}	10^2	$1.4*10^{1}$	$4.3*10^{-12}$
	10^3	$9.0*10^{1}$	$2.0*10^{-11}$
	10^4	$1.4*10^{3}$	$2.0*10^{-10}$
⑥ 10^{-11}	10^2	$4.2*10^{1}$	$4.3*10^{-13}$
	10^3	$6.0*10^{2}$	$2.0*10^{-12}$
	10^4	$9.0*10^{3}$	$2.0*10^{-11}$
⑦ 10^{-12}	10^2	$2.7*10^{2}$	$4.3*10^{-14}$
	10^3	$4.0*10^{3}$	$2.0*10^{-13}$
	10^4	$5.9*10^{4}$	$2.0*10^{-12}$

Figure 5. Helium Wave-front Velocity, Location and Average Pressure in a 6.9 cm ϕ Cold-Bore Tube with no Pumps, at 4.2 K and for Various Leak Rates.

Kimo M. Welch
August 17, 1992

"velocity"
0.4=1; 2,1.5

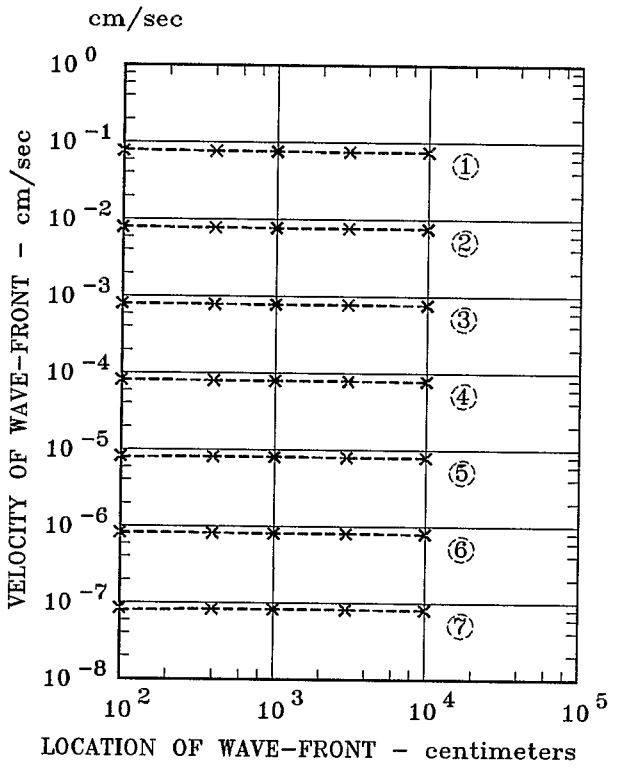

Q Total Torr-L/sec	Wave-Front Location-cm	Time to x - days	Average Interval Pressure - Torr
① 10^{-6}	10^2	$2.7*10^{-3}$	$3.0*10^{-8}$
	10^3	$4.1*10^{-2}$	$1.4*10^{-7}$
	10^4	$6.6*10^{-1}$	$1.4*10^{-6}$
② 10^{-7}	10^2	$1.7*10^{-2}$	$3.0*10^{-9}$
	10^3	$2.6*10^{-1}$	$1.4*10^{-8}$
	10^4	$4.1*10^{0}$	$1.4*10^{-7}$
③ 10^{-8}	10^2	$1.1*10^{-1}$	$3.0*10^{-10}$
	10^3	$1.6*10^{0}$	$1.4*10^{-9}$
	10^4	$2.6*10^{1}$	$1.4*10^{-8}$
④ 10^{-9}	10^2	$6.6*10^{-1}$	$3.0*10^{-11}$
	10^3	$1.0*10^{1}$	$1.4*10^{-10}$
	10^4	$1.6*10^{2}$	$1.4*10^{-9}$
⑤ 10^{-10}	10^2	$4.1*10^{0}$	$3.0*10^{-12}$
	10^3	$6.3*10^{1}$	$1.4*10^{-11}$
	10^4	$1.0*10^{3}$	$1.4*10^{-10}$
⑥ 10^{-11}	10^2	$2.6*10^{1}$	$3.0*10^{-13}$
	10^3	$3.9*10^{2}$	$1.4*10^{-12}$
	10^4	$6.2*10^{3}$	$1.4*10^{-11}$
⑦ 10^{-12}	10^2	$1.6*10^{2}$	$3.0*10^{-14}$
	10^3	$2.5*10^{3}$	$1.4*10^{-13}$
	10^4	$3.9*10^{4}$	$1.4*10^{-12}$

Figure 6. Hydrogen Wave-front Velocity, Location and Average Pressure in a 6.9 cm ϕ Cold-Bore Tube with no Pumps, at 4.2 K and for Various Leak Rates.

Kimo M. Welch
August 17, 1992

"velocity"
0.4=1; 2,1.5

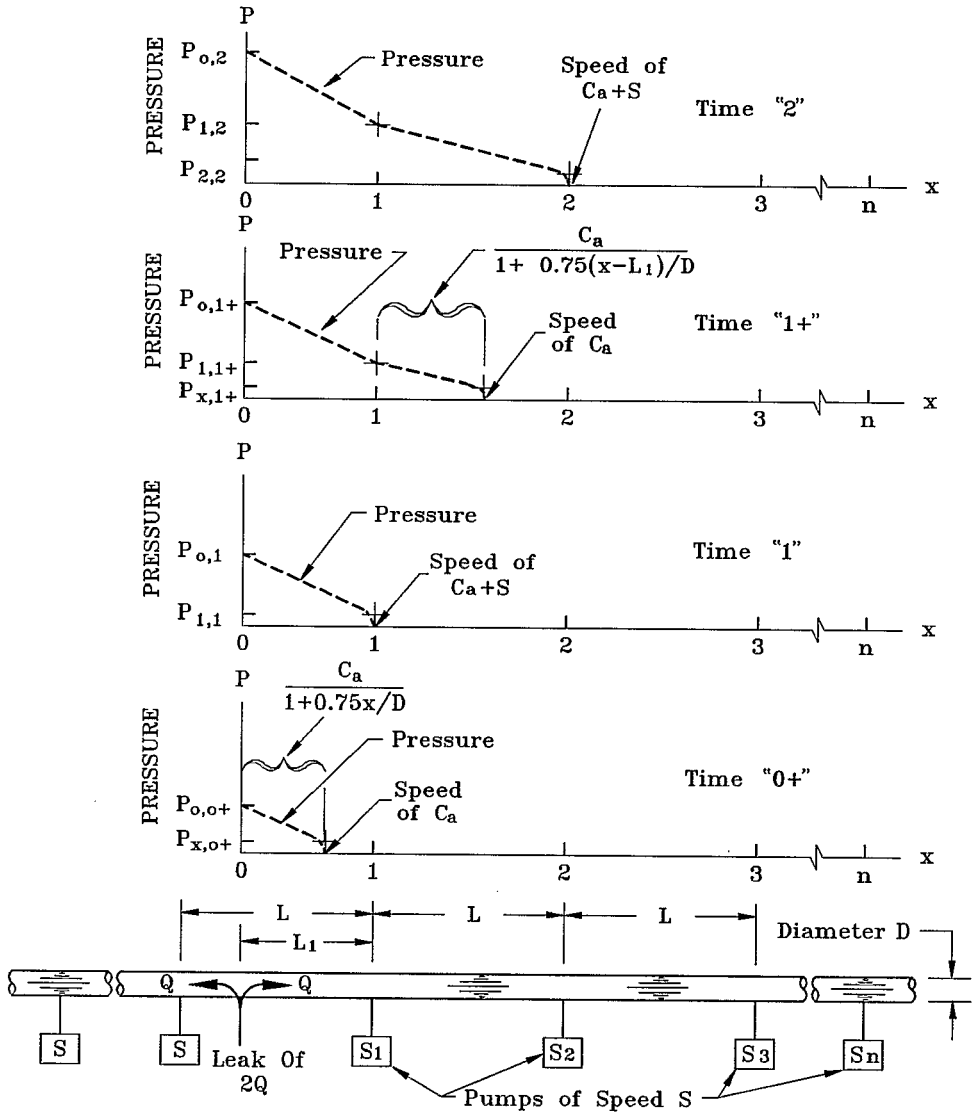

Figure 7. Gas Wave-front Propagation in Cold-bore Pipe.

kimo
"coldbore"
1.5,1.5; 0.5=1

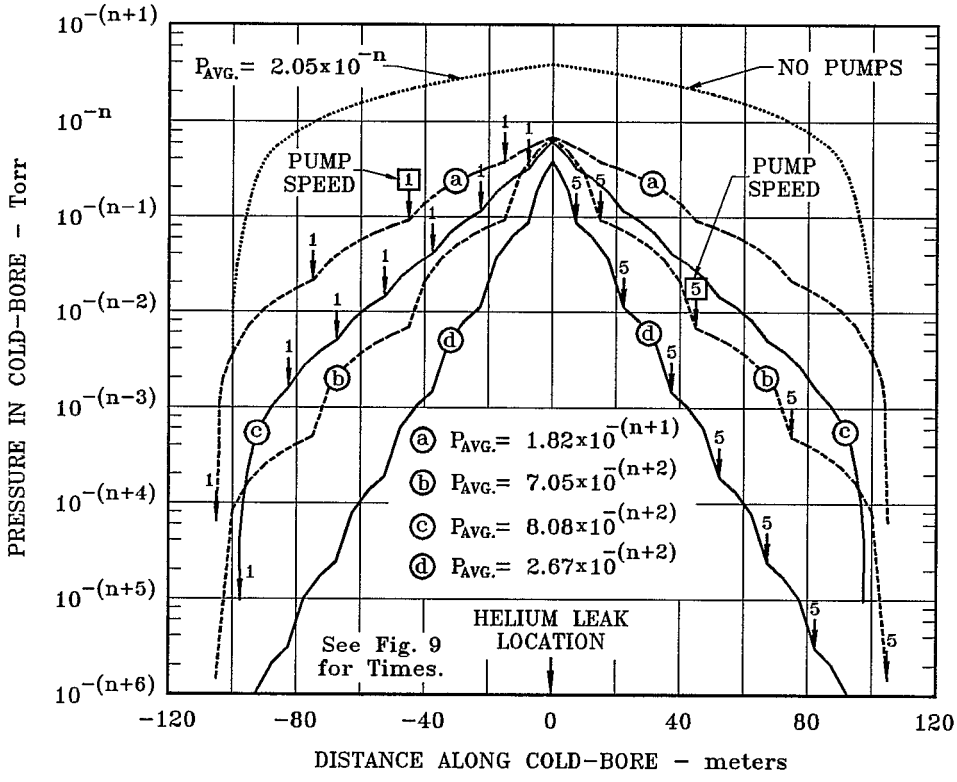

Figure 8. Helium Pressure Profiles at Different Times in a 6.9 cm ϕ Cold-Bore Tube at 4.2 K, for a Leak Rate of 10^{-n} Torr-Liters/sec and for Pumps of Two Speeds and Spaced at Intervals of 15 & 30 m.

"hepress"
Kimo M. Welch
August 11, 1992
1.5,3; 0.5=1

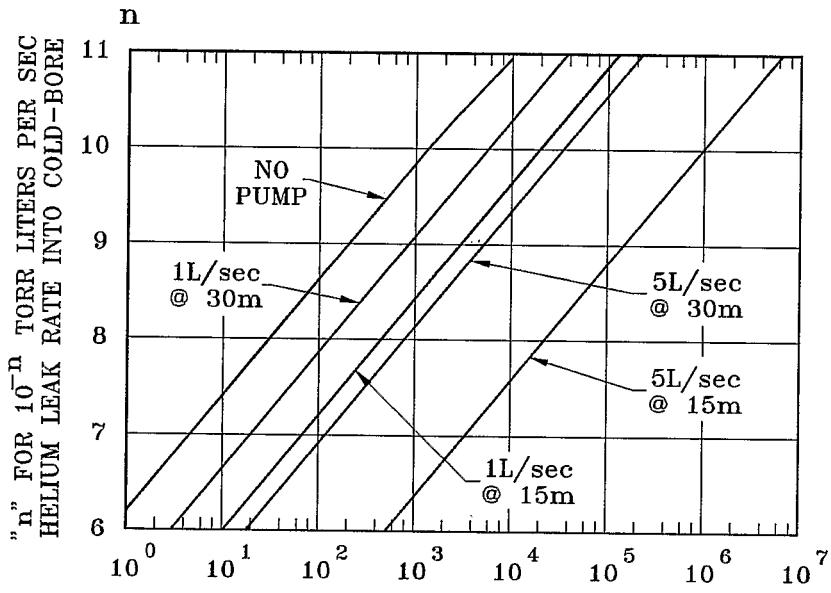

Figure 9. Time of Helium Wave-Front Propagation in 4.2 K Cold-Bore vs. Pump Speed and Interval of Pump Spacing.

"deltalsn"
Kimo M. Welch
August 5, 1992
1.75,3; 0.5=1

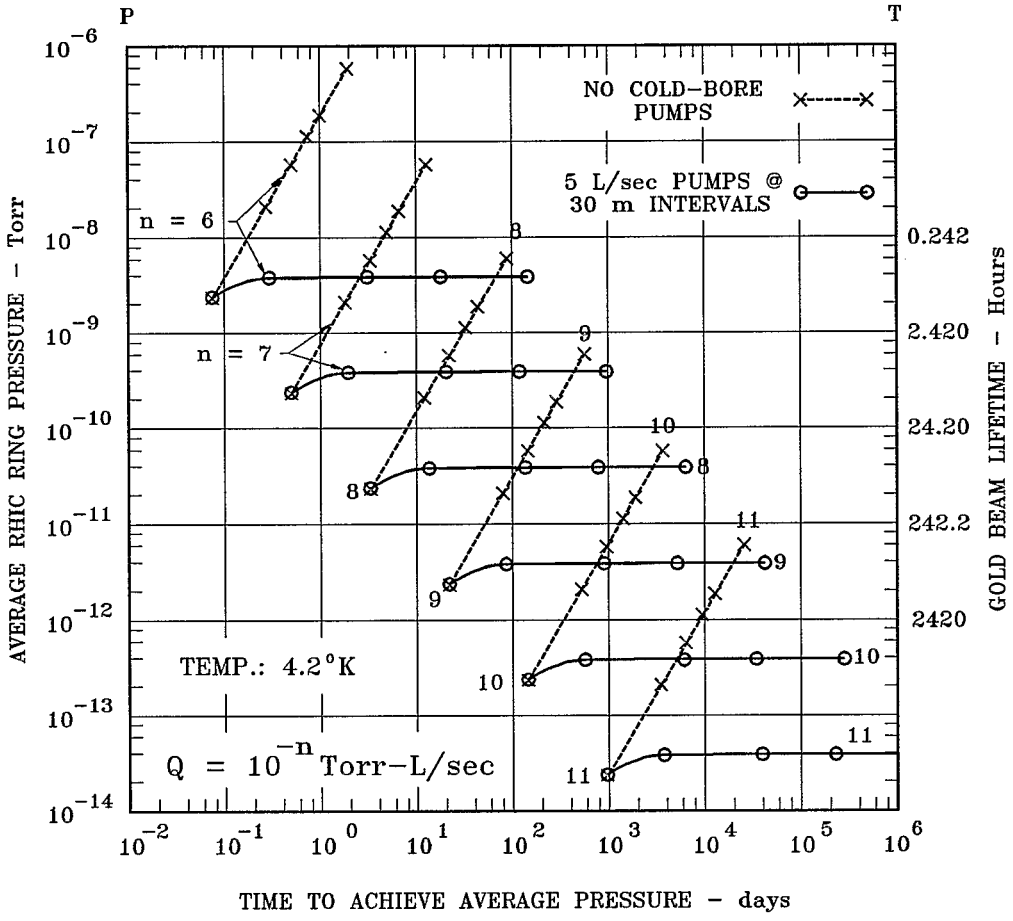

Figure 10. Average Pressure and Gold Beam Lifetimes in One RHIC Ring Due to One Helium Leak of Magnitude 10^{-n} Torr-L/sec in the 6.9 cm ϕ Beam Tube.

"pbarrhic"
Kimo M. Welch
August 12, 1992
1.5,2; 0.5=1

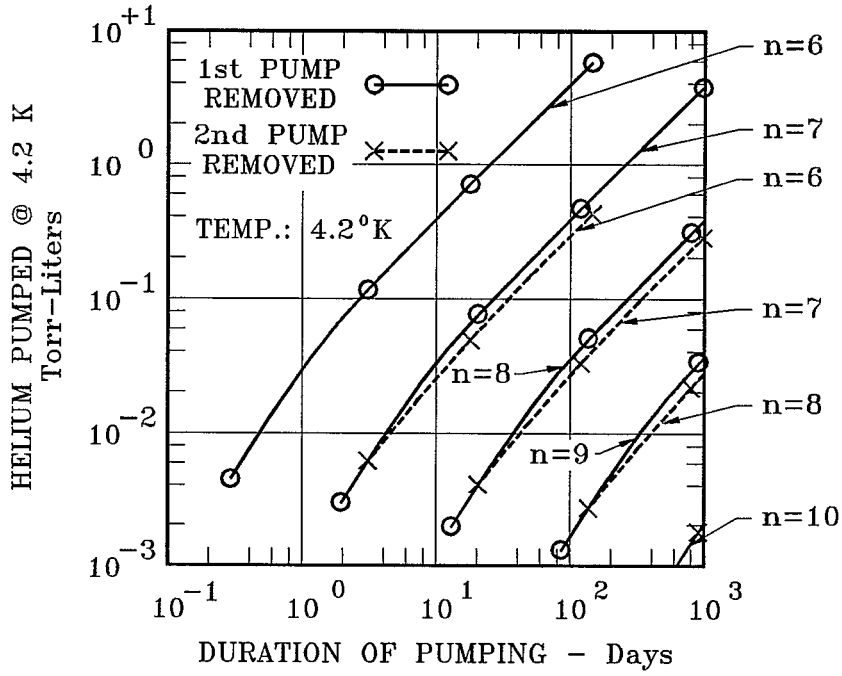

Figure 11. Amount of Helium Pumped by Pumps Spaced at 30 meter Intervals along a 6.9 cm ϕ Cold-Bore and Pumping on a Leak Rate of 10^{-n} Torr-Liters/sec.

"pvinpump"
Kimo M. Welch
August 16, 1992
1.5,3; 0.7=1

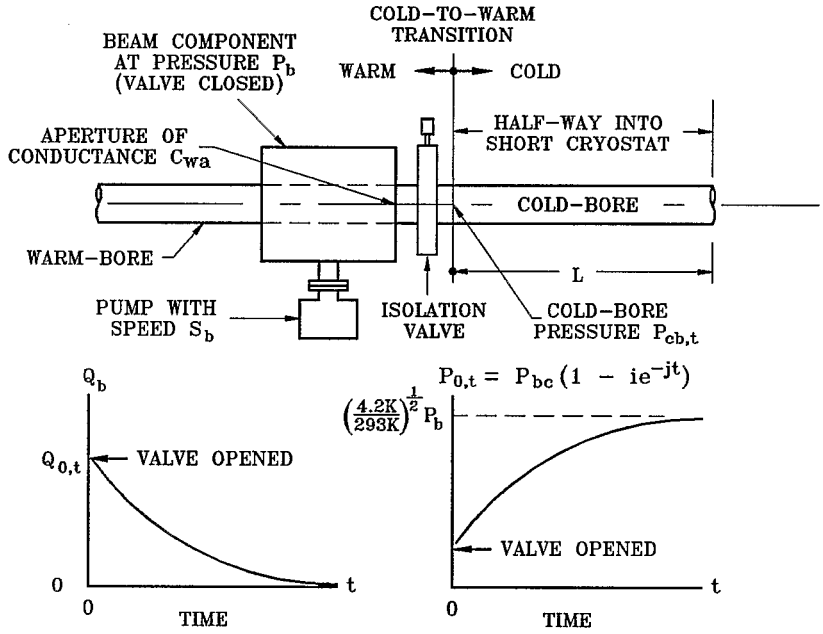

Figure 12. Hydrogen Pumping by the Cold–Bore as a Function of Time as a Consequence of Opening the Warm–to–Cold Isolation Valve.

"h2endeff"
Kimo M. Welch
August 5, 1992
1.750,3; 0.4=1